Original Research

Sex-specific differences in the gut microbiota and fecal metabolites in an adolescent valproic acid-induced rat autism model

You-Yu Gu[1], Ying Han[2,*], Jing-Jing Liang[1], Ya-Nan Cui[1], Bi Zhang[1], Ying Zhang[1], Shao-Bin Zhang[3], Jiong Qin[1,*]

[1]*Department of Pediatrics, Peking University People's Hospital, 100044 Beijing, China,* [2]*Department of Pediatrics, Peking University First Hospital, 100034 Beijing, China,* [3]*Beijing Gutgene Technology Co. Ltd, 100085 Beijing, China*

TABLE OF CONTENTS

1. Abstract

Background: Alterations in the microbiota-gut-brain axis are associated with the onset of autism spectrum disorder (ASD). Numerous studies have reported that the gut microbiota (GM) is significantly altered in individuals with ASD and animal models of ASD. However, few studies have focused on sex-specific differences in the GM and fecal metabolites of ASD. **Methods**: In this study, we performed 16S rRNA gene sequencing and untargeted metabolomics in parallel on fecal samples from a valproic acid (VPA)-induced rat model of autism (VPA rats). Based on these data, we analyzed differentially abundant metabolites in the Kyoto Encyclopedia of Genes and Genomes (KEGG) database to reveal the possible mechanism of ASD. Data derived from male and female rats were analyzed separately. Finally, we analyzed the correlation between characteristic genera and characteristic fecal metabolites in VPA rats of both sexes. **Results**: The results showed that VPA rats of both sexes presented remarkable alterations in the GM and fecal metabolites. Sex-specific differences were noticeably detected. We identified 51 annotated differentially abundant fecal metabolites and 1 differentially enriched KEGG pathway between the male VPA and male control groups. *Ruminococcus_2*, *Candidatus_Soleaferrea*,

Submitted: 23 August 2021 Revised: 23 September 2021 Accepted: 30 October 2021 Published: 30 December 2021

Desulfovibrio, *Candidatus_Saccharimonas*, *Intestinimonas*, *[Eubacterium]_xylanophilum_group*, *[Eubacterium]_brachy_group* and *[Bacteroides]_pectinophilus_group* were the characteristic genera of male VPA rats. Between the female VPA and female control groups, 124 annotated differentially abundant fecal metabolites were identified without differentially enriched KEGG pathways. *Ruminiclostridium*, *Acetatifactor*, *Desulfovibrio*, *[Eubacterium]_xylanophilum_group* and *Candidatus_Saccharimonas* were the characteristic genera of female VPA rats. Correlation analysis revealed a tight relationship between the GM and fecal metabolites in VPA rats of both sexes. **Conclusions**: In conclusion, alterations in the GM and fecal metabolites in VPA rats showed sex-specific differences. The therapy for ASD might be different between sexes in the future.

2. Introduction

Autism spectrum disorder (ASD) is an intractable neurodevelopmental disability caused by multiple genetic and environmental factors [1–3]. The characteristic symptoms of ASD include social deficits and repetitive behaviors [4]. In recent years, the prevalence of ASD has grown very rapidly in industrialized countries [5]. However, the mechanism of ASD remains unclear with no effective medications. The morbidity of ASD is typically male biased, with a male-to-female ratio of approximately 4 to 1 [6, 7]. A previous study also reported that the mechanism of ASD is different between sexes [8]. Thus, sex-specific studies may help better illuminate the mechanisms of ASD.

The "microbiota-brain-gut axis" theory has been well acknowledged [9]. The gut microbiota (GM) is able to communicate with the central nervous system (CNS), modulate brain functions and influence individual behaviors [10]. GM produced a set of metabolites present in the feces. These metabolites were defined as fecal metabolites, which could partly reflect the GM status and the relationship between the GM and host [11]. The GM communicates with the CNS via gut hormones, the vagus nerve, the immune system and fecal metabolites [12]. On the other hand, signals from the CNS can affect the number and composition of GM constituents and fecal metabolites [13]. Thus, the detection and analysis of GM and fecal metabolites might be an effective strategy to explore the mechanism of intractable CNS disorders.

Recently, the GM has been suggested to be involved in the pathogenesis of ASD due to the frequent occurrence of gastrointestinal (GI) dysfunctions in ASD patients [14–20]. A large number of papers have revealed that the GM is significantly altered in patients with ASD or animal models of ASD when compared with that in their controls [21–34]. Colonization with GM from ASD individuals is sufficient to induce hallmark autistic behaviors in mice [35]. Fecal metabolites are also altered in children with ASD [26, 36, 37]. For example, serotonin plays as a link between the gut-brain-microbiome axis in the pathogenesis of ASD [38]. Indigenous bacteria from the GM can regulate host serotonin biosynthesis [39]. However, the results from different trials were inconsistent because of the heterogeneity of age, sex, race, and severity of GI symptoms and the differences in detection methods. According to the latest studies, 16S rRNA gene sequencing and ultra-high-performance liquid chromatography/mass spectrometry (UHPLC-MS) based untargeted metabolomics might be useful methods to detect the true variations in the GM and fecal metabolites, respectively [40]. To our knowledge, UHPLC-MS based untargeted metabolomics has seldom or never been used in fecal samples of ASD patients or animal models.

Valproic acid (VPA) is a commonly used antiepileptic drug in the clinic. A single intraperitoneal injection of VPA during the second trimester in female rats is well accepted to establish a rat autism model in offspring (VPA rats). This animal model manifests typical autism-like behaviors, including deficits in social interaction and neurodevelopment, increased repetitive behavior and reduced pain sensitivity [41]. The level of 5-hydroxytryptamine (5-HT) is increased in the brain and reduced in peripheral blood [42]. In addition, the alterations of the GM in VPA rats are similar to those in ASD patients [43]. Overall, VPA rats might be suitable to explore the true variations in the GM and fecal metabolites in ASD.

In this study, 16S rRNA gene sequencing and UHPLC-MS based untargeted metabolomics were performed to explore the taxonomical characterization of GM and the features of fecal metabolites in VPA rats. Based on these data, we explored the potential mechanism of ASD induced by prenatal exposure to VPA. In addition, we addressed the sex-specific differences due to the male-biased morbidity of ASD.

3. Materials and methods

3.1 Animals

Eight male and eight female Wistar rats aged 10–12 weeks and weighing 270–290 g were purchased from Vital River Laboratory Animal Technology (Beijing, China). The animals were housed at 23 ± 2 °C and 50% ± 10% humidity under a 12-h light/dark cycle. The experimental procedures were in line with the USA National Institutes of Health Guide for the Care and Use of Laboratory Animals and approved by the Animal Care and Use Committee of Peking University People's Hospital (2019PHE007).

3.2 Construction of the VPA-induced rat model of autism

We constructed the animal model in accordance with previous studies [44, 45]. Female rats were paired with

male rats overnight. The day after a vaginal plug was detected was considered embryonic day 0.5 (E 0.5). Pregnant rats were housed individually and randomly distributed into two groups: the VPA-treated group (n = 4) and the normal saline (NS) group (n = 4). Pregnant rats in the VPA-treated group were intraperitoneally injected with VPA (Sigma: P4543) at a dose of 600 mg/kg on E 12.5. In the NS group, the rats received the same volume of NS. After weaning at postnatal day 21 (PND 21), every 4-5 pups of the same group and sex were raised in the same cage until the end of fecal sample collection.

3.3 Experimental groups

We randomly selected 1 male and 1 female pup from each litter for our experiment. A total of 16 pups from litters in the VPA-treated group and NS group were included and divided into 4 groups, with 4 animals each: the (1) male control group (mCtrl group), (2) male VPA group (mVPA group), (3) female control group (fCtrl group), and (4) female VPA group (fVPA group).

3.4 Collection of feces

Pups were individually placed into clean cages. After defecation, we used sterile tweezers to collect the fecal pellets into sterile cryotubes and immediately transferred them into liquid nitrogen. After collection of feces, all the fecal samples were stored at –80 °C until analysis by untargeted metabolomics and 16S rRNA sequencing.

3.5 16S rRNA gene sequencing

16S rRNA gene sequencing was performed based on the method described previously with some modifications [46]. Total fecal genomic DNA was extracted with an E.Z.N.A Stool DNA Kit (OMEGA, USA) and quantified by a Nanodrop 2000 spectrophotometer (Thermo Fisher Scientific, Waltham, MA, USA). The V3-V4 region of the 16S rRNA gene was amplified with the primers 341F (5′-CCTAYGGGRBGCASCAG-3′) and 806R (5′-GGACTACNNGGGTATCTAAT-3′). Twenty microliter PCR mixtures were set up with 4 μL 5×FastPfu buffer, 2 μL deoxynucleoside triphosphates (dNTPs) (2.5 mM), 0.8 μL each primer, 0.4 μL FastPfu polymerase, and template DNA (10 ng). PCR was performed in a GeneAmp 9700 (ABI) thermocycler (Thermo Fisher Scientific, Waltham, MA, USA) with Phusion High-Fidelity PCR Master Mix. The parameters were set as follows: initial denaturation at 95 °C for 5 min; 27 cycles of denaturation at 95 °C for 30 s, annealing at 55 °C for 30 s, and elongation at 72 °C for 45 s; and an additional elongation at 72 °C for 10 min.

PCR products were detected by 2% agarose gel electrophoresis and purified by a quick gel extraction kit (Qiagen, Dusseldorf, Germany). Library pools were produced with equal amounts of PCR products with a TruSeq Nano DNA LT sample prep kit (Illumina, San Diego, California, USA); these pools were amplified through paired-end sequencing on the Illumina MiSeq PE300 platform.

The quality control (QC) of original data was carried out using Trimmomatic v0.39 software (http://www.usadellab.org/cms/index.php?page=trimmomatic). Based on the overlap (minimum: 10 bp) between paired-end (PE) reads after QC, PE reads were assembled using Flash v1.2.11 software (McKusick-Nathans Institute of Genetic Medicine, Johns Hopkins University School of Medicine, USA). QIIME v1.9.1 software (Knight Lab in University of California, San Diego, USA) (QIIME allows analysis of high-throughput community sequencing data) was adopted for processing, and VSEARCH v2.14.1 software (Department of Informatics, University of Oslo, Norway) (VSEARCH: a versatile open-source tool for metagenomics) was used to detect chimera sequences. We used the Uclust method in the QIIME v1.9.1 software package to perform operational taxonomic units (OTUs) clustering analysis according to 97% sequence similarity level. Rarefaction was not applied in our research. On the basis of the Silva database Release 138 (http://www.arb-silva.de), taxonomic annotations were made for the OTUs of each sample using a confidence threshold of 70%. LefSe (http://huttenhower.sph.harvard.edu/galaxy/root?tool_id=lefse_upload) was used to evaluate the effect of each taxon on discrimination between different groups. The Shannon, Simpson, Chao1 and ACE indices of microbial communities were calculated by Mothur (https://mothur.org/). Principal coordinates analysis (PCoA), based on Bray-Curtis dissimilarity, was analyzed by permutational multivariate analysis of variance (PERMANOVA) in R language v3.2.1 (University of Auckland, New Zealand) to determine the different bacterial communities of beta-diversity.

3.6 UHPLC-MS based untargeted metabolomics

Fecal samples (100 mg each sample) were triturated in liquid nitrogen and vortexed with 300 μL lysis buffer (80% methanol solution). The mixtures were homogenized at 45 Hz for 4 min and ultrasonicated at 4 °C and 40 kHz for 5 min. Then, we placed the mixtures at –20 °C for 30 min and centrifuged at 4 °C and 14000 × g for 30 min. The supernatant of each sample was collected for UHPLC-MS analysis. The column was a ACQUITY UPLC HSS T3 column (100 mm × 2.1 mm i.d., 1.8 μm; Waters). The mobile phase A was water (containing 0.1% formic acid), and the mobile phase B was acetonitrile (contains 0.1% formic acid). The flow rate, injection volume, and column temperature were 0.25 mL/min, 5 μL, and 35 °C, respectively. A QC sample (prepared after metabolite extraction, mixing equal volumes of all samples) was used to evaluate the stability of the analytical system and ensure the reliability of the results.

UHPLC-MS was performed on a UPLC I-class instrument (Waters, ACQUITY UPLC). It was equipped with a binary solvent delivery manager, an autosampler and a mass spectrometer (Waters, Vion IMS QTof) with an electrospray interface. Sample mass spectrometric data were

collected in either positive or negative ionization mode. We set the source temperature, desolvation temperature and desolvation gas flow to 120 °C, 500 °C and 800 L/h, respectively. Centroid data were assembled from 100–1200 *m/z* with a 0.3 s scan time. The capillary voltages were 3.2 kV and –2.2 kV in positive ionization mode and negative ionization mode, respectively. Before pattern recognition, the original data were subjected to preprocessing. Baseline filtering, peak identification, integration, retention time correction, peak alignment and normalization were performed using Progenesis QI 2.3 software. Then, the METLIN database (https://metlin.scripps.edu), Human Metabolome database (http://www.hmdb.ca/) and ChemSpider database (www.chemspider.com) were applied for metabolite annotation. The fragmentation mass spectrum of metabolites was matched to fragmentation mass spectra in library and scored. The results with higher score were accepted as the identification results.

Principal component analysis (PCA) and orthogonal partial least squares discrimination analysis (OPLS-DA), performed by the SIMCA-P software package (v13.0, Umetric, Umea◦, Sweden), were used to observe the degree of dispersion and distinguish the overall differences in metabolic profiles, respectively. In OPLS-DA model, metabolites with variable importance in projection (VIP) >1 were set as differential variables [47, 48]. The method of 100 replacement tests was carried out to examine the fitting effect of OPLS-DA and prevent the model from overfitting. Variables with VIP >1.0 and $p < 0.05$ calculated by Student's *t*-test were defined as differential metabolites. All differentially abundant metabolites were annotated in pathways in the Kyoto Encyclopedia of Genes and Genomes (KEGG) database (http://www.genome.jp/kegg/) [49]. Pathway enrichment analysis was performed using the Python software package (https://docs.scipy.org/doc/scipy/). Receiver operator characteristic (ROC) analysis was carried out using R language (version 3.2.1) to calculate the area under the curve (AUC) and evaluate the degree of influence of metabolites on the distinction between the VPA and Ctrl groups in different sexes.

3.7 Statistical analysis

Quantitative sequencing data with a nonnormal distribution were analyzed by the Wilcoxon rank sum test, and *p*-values were checked using the Benjamini Hochberg false discovery rate (FDR). Data were presented as the mean ± standard deviation (SD). The Pearson correlation coefficient was used to express the correlation degree between characteristic genera and characteristic fecal metabolites. GraphPad Prism 8.0.1 software (GraphPad Software, San Diego, California, USA) was used for data analysis and graphing. A double-tailed $p < 0.05$ was accepted as statistically significant.

4. Results

4.1 Taxonomical characterization of the gut microbiota in male and female VPA rats

To detect the taxonomical characterization of the GM in male and female VPA rats, fecal samples were analyzed by 16S rRNA gene sequencing. We obtained 943,972 sequences and 390,572,407 bases from 16 samples with an average of 58,998 sequences per sample. A total of 1501 OTUs were annotated in all samples (1501 at the phylum level; 1499 at the class level; 1496 at the order level; 1448 at the family level; 861 at the genera level; 115 at the species level). The analysis of α-diversity showed no significant differences in either sex between Ctrl and VPA rats using the Chao1 estimator (Fig. 1A), ACE estimator (Fig. 1B), Shannon index (Fig. 1C) and Simpson index (Fig. 1D). PCoA showed that the overall composition of the GM was not different between the mCtrl and mVPA groups (R = 0.193, $p = 0.151$, Fig. 1E), while between the fCtrl and fVPA groups, the overall composition of the GM was significantly different (R = 0.267, $p = 0.036$, Fig. 1E). At the phylum level, the mVPA group showed an increased Firmicutes/Bacteroides (F/B) ratio compared with that of the mCtrl group (Fig. 1F), while the fVPA group showed a decreased F/B ratio compared with that of the fCtrl group (Fig. 1F). The LefSe results showed that at the genus level, *Ruminococcus_2*, *Candidatus_Soleaferrea*, *Desulfovibrio*, *Candidatus_Saccharimonas*, *Intestinimonas*, *[Eubacterium]_xylanophilum_group*, *[Eubacterium]_brachy_group* and *[Bacteroides]_pectinophilus_group* were characteristic genera in the mVPA group (Fig. 1G), while *Ruminiclostridium*, *Acetatifactor*, *Desulfovibrio*, *[Eubacterium]_xylanophilum_group* and *Candidatus_Saccharimonas* were characteristic genera in the fVPA group (Fig. 1H). The relative abundances of characteristic genera of either sex of VPA rats showed no significant differences (Tables 1,2). These results revealed the taxonomical characterization of GM constituents in male and female VPA rats, with obvious sex-specific differences.

4.2 Characteristics of fecal metabolites in male and female VPA rats

Untargeted metabolomics was performed to investigate the characteristic fecal metabolites in male and female VPA rats. PCA (Fig. 2A–D), OPLS-DA (Fig. 2E–H) and model validation (Fig. 2I–L) revealed that in both sexes, the distribution of samples between VPA and Ctrl rats was different, implying a significant difference in fecal metabolites. Between the mCtrl and mVPA groups, we detected 51 annotated differentially abundant metabolites (Fig. 2M,N, **Supplementary Table 1**). A total of 124 annotated differentially abundant metabolites were detected between the fCtrl and fVPA groups (Fig. 2O,P, **Supplementary Table 2**). Detailed information on these annotated differentially

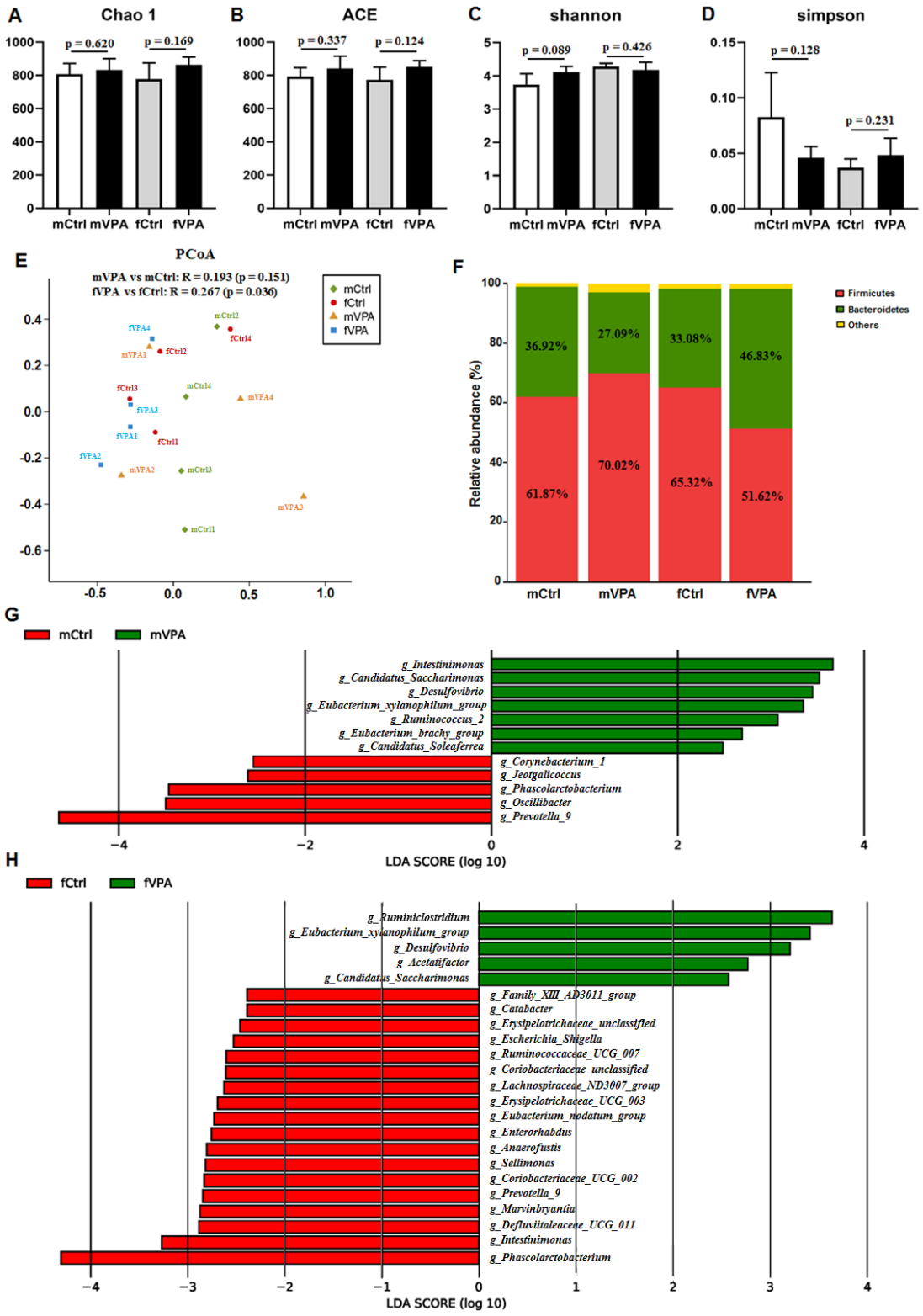

Fig. 1. The difference in gut microbiota in different sexes between the Ctrl and VPA rats. (A) Chao1 index. (B) ACE index. (C) Shannon index. (D) Simpson index. (E) PCoA chart. The X and Y axes represent two selected principal axes. The percentage represents the explanatory value of the principal axis for the difference between samples. (F) Column chart of species composition at the phylum level. (G–H) LDA chart. The impact of the representative species abundance on the differences between (G) the mVPA and mCtrl groups or between (H) the fVPA and fCtrl groups. mCtrl, male control group; mVPA, male VPA group; fCtrl, female control group; fVPA, female VPA group.

Table 1. The relative abundances of characteristic genera (mVPA vs mCtrl group).

	mVPA (mean)	mVPA (SD)	mCtrl (mean)	mCtrl (SD)	*p*-value	FDR
Ruminococcus_2	0.00262	0.00310	0.00020	0.00011	0.0294	0.5776
Candidatus_Soleaferrea	0.00061	0.00041	7.76×10^{-5}	4.24×10^{-5}	0.0294	0.5776
Desulfovibrio	0.00609	0.00224	0.00047	0.00047	0.0304	0.5776
Candidatus_Saccharimonas	0.00713	0.00730	0.00020	0.00021	0.0304	0.5776
Intestinimonas	0.01044	0.01141	0.00165	0.00130	0.0606	0.5776
[Eubacterium]_xylanophilum_group	0.00509	0.00312	0.00083	0.00120	0.0606	0.5776
[Eubacterium]_brachy_group	4.43×10^{-5}	3.62×10^{-5}	0	0	0.0668	0.5776
[Bacteroides]_pectinophilus_group	0.00026	0.00031	0	0	0.0689	0.5776

mVPA, male VPA group; mCtrl, male control group; SD, standard deviation; FDR, false discovery rate.

Table 2. The relative abundances of characteristic genera (fVPA vs fCtrl group).

	fVPA (mean)	fVPA (SD)	fCtrl (mean)	fCtrl (SD)	*p*-value	FDR
Ruminiclostridium	0.01217	0.01614	0.00103	0.00031	0.0304	0.2582
Acetatifactor	0.00176	0.00097	0.00049	0.00026	0.0304	0.2582
Desulfovibrio	0.00274	0.00349	0.00041	0.00036	0.0591	0.2582
[Eubacterium]_xylanophilum_group	0.00646	0.00402	0.00114	0.00194	0.0606	0.2582
Candidatus_Saccharimonas	0.00089	0.00054	0.00021	0.00020	0.0606	0.2582

fVPA, female VPA group; fCtrl, female control group; SD, standard deviation; FDR, false discovery rate.

abundant metabolites is shown in **Supplementary Table 1** and **Supplementary Table 2**. These results indicated that fecal metabolite levels were altered in both sexes of adolescent VPA rats.

4.3 Differential metabolites and KEGG pathways in male and female VPA rats

We further analyzed these annotated differentially abundant metabolites in KEGG pathways. Between the mVPA and mCtrl groups, among the 51 annotated differentially abundant metabolites, 7 metabolites participated in 10 specific KEGG pathways (Table 3, Fig. 3A) and were significantly enriched in 1 KEGG pathway named the pathway for cyanoamino acid metabolism (p = 0.0027, FDR = 0.0159, Fig. 3A). Among the 7 metabolites, we focused on 4 metabolites with VIP >2 (Table 3). ROC analysis showed that the AUC values of these 4 metabolites were larger than 0.85 (Fig. 3B–E), suggesting their potential as important biological indicators to distinguish between the mVPA and mCtrl groups. Between the fVPA and fCtrl groups, among the 124 annotated differentially abundant metabolites, 15 metabolites participated in 34 specific KEGG pathways (Table 4, Fig. 4A). However, these metabolites were not significantly enriched in any KEGG pathways (Fig. 4A). Among the 15 metabolites, we focused on 8 metabolites with VIP >2 (Table 4). ROC analysis showed that the AUC values of these 8 metabolites were larger than 0.85 (Fig. 4B–I), suggesting their potential as important biological indicators to distinguish between the fVPA and fCtrl groups. These results revealed the potential mechanism of ASD induced by prenatal exposure to VPA as well as the characteristic fecal metabolites of male and female adolescent VPA rats. Sex-specific differences were obvious among these results.

4.4 Correlation between characteristic genera and characteristic fecal metabolites in male and female VPA rats

We used Pearson correlation coefficients to assess the correlation between characteristic genera and fecal metabolites. Fig. 5A shows the correlation between 4 characteristic metabolites and 8 characteristic genera in male VPA rats. The abundance of hesperetin and protoanemonin negatively correlated with that of *Candidatus_Soleaferrea* and *Desulfovibrio*. In addition, the abundance of protoanemonin negatively correlated with that of *Ruminococcus_2*. Fig. 5B shows the correlation between 8 characteristic metabolites and 5 characteristic genera in female VPA rats. The abundance of *Ruminiclostridium*, *Acetatifactor* and *[Eubacterium]_xylanophilum_group* positively correlated with that of brassicasterol, allocholic acid, palmitoyl glucuronide and D-1-piperideine-2-carboxylic acid but negatively correlated with that of 4-(methylnitrosamino)-1-(3-pyridyl)-1-butanol. The abundance of *Acetatifactor* and *[Eubacterium]_xylanophilum_group* positively correlated with that of LysoPC(14:1(9Z)) but negatively correlated with that of androstenedione. In addition, the abundance of cis-acetylacrylate negatively correlated with that of *Ruminiclostridium*, *Acetatifactor* and *Candidatus_Saccharimonas*. Correlation analysis revealed a tight relationship between the GM and fecal metabolites in VPA rats of both sexes. The results of the correlation between characteristic genera and characteristic fecal metabolites in VPA rats also showed sex-specific differences.

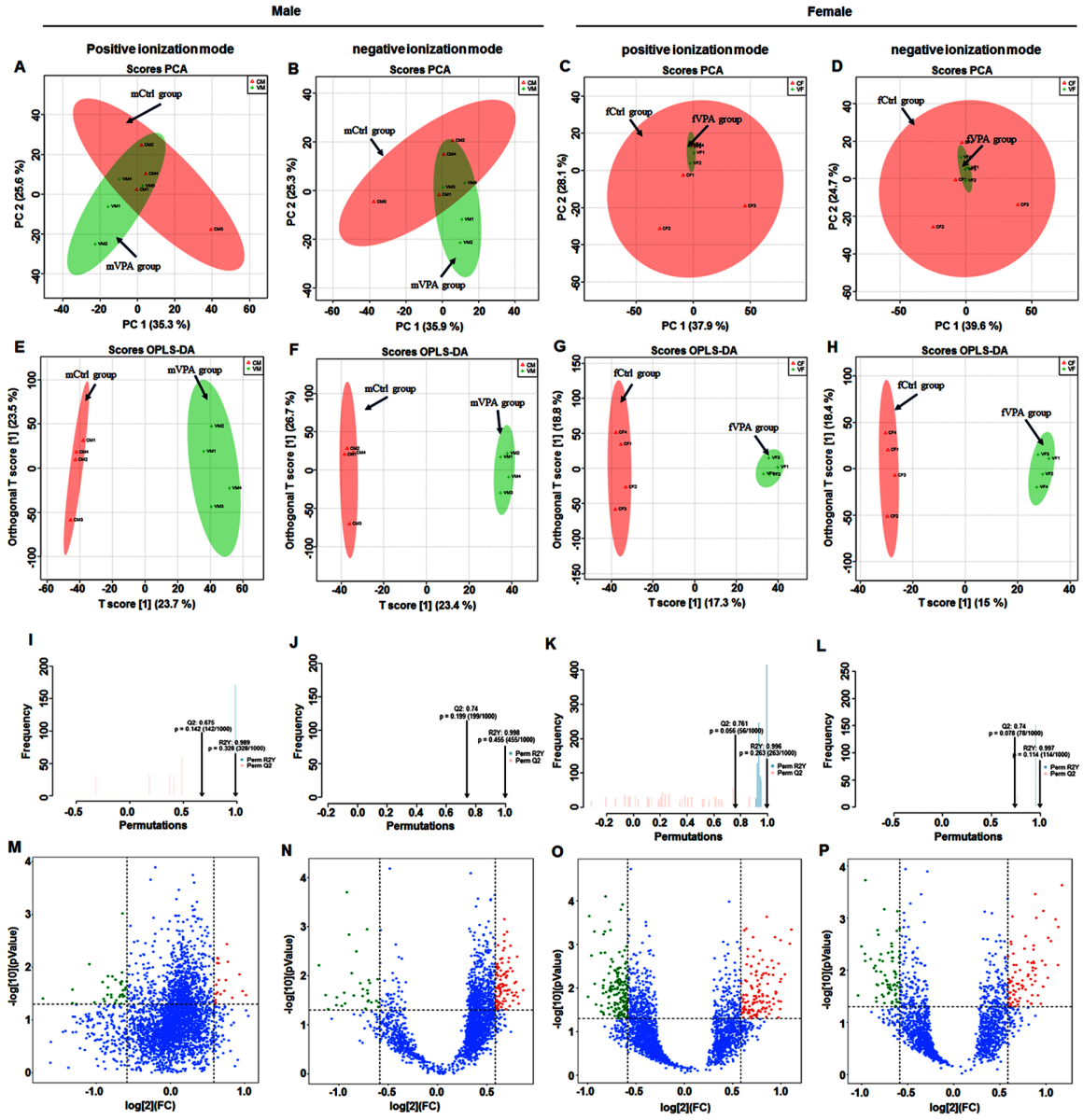

Fig. 2. The difference in fecal metabolites in different sexes between the Ctrl and VPA rats. (A–D) Principal component analysis (PCA). (E–H) Orthogonal partial least squares discrimination analysis (OPLS-DA). (I–L) OPLS-DA model validation. (M–P) Volcano map of differentially abundant metabolites. mCtrl, male control group; mVPA, male VPA group; fCtrl, female control group; fVPA, female VPA group.

5. Discussion

Sex-specific differences have been found in many diseases. Among these diseases, ASD is well acknowledged because of the typically male-biased morbidity [6, 7]. Coretti *et al.* [33] investigated sex-related alterations in GM composition in BTBR mice, a well-established mouse model of autism. They detected sex-related differences in BTBR mice and identified *Bacteroides*, *Parabacteroides*, *Sutterella*, *Dehalobacterium* and *Oscillospira* as key genera of sex-specific GM profiles. Foley *et al.* [50] found that adolescent male rats prenatal exposure to propionic acid showed increased levels of locomotor activity compared with female rats. These results suggested that the mechanism of ASD is different between sexes. However, to our knowledge, few studies have investigated the sex-specific differences in GM and fecal metabolites as well as the underlying mechanisms in individuals with ASD or other animal models of ASD. These problems need to be deeply explored.

A single intraperitoneal injection of VPA in the second trimester of pregnant rats is well known to establish a rat autism model in offspring [44, 45]. This model manifests characteristic autism symptoms and has been widely accepted to be useful for exploration of the pathogenesis of ASD [51–54]. Recently, Liu *et al.* [43] investigated the taxonomical characterization of the GM in male and female

Table 3. Relative abundance of 7 significant differential metabolites involved in KEGG pathway analysis between mCtrl and mVPA group (Mean ± SD).

Description	kegg_id	ESI mode	*m/z*	mCtrl	mVPA	VIP	FC	*p*-value	State	AUC
Melphalan	C07122	neg	303.0671	7333 ± 1599	4264 ± 855	2.41	1.61	0.0250	down	0.9375
Hesperetin	C01709	neg	301.0731	9207 ± 1153	5515 ± 911	2.35	1.52	0.0070	down	1
Protoanemonin	C07090	pos	97.0288	54478 ± 11926	31607 ± 1828	2.29	1.71	0.0079	down	1
Linamarin	C01594	pos	248.1128	527502 ± 104435	330320 ± 57829	2.01	1.65	0.0280	down	0.875
gamma-Glutamyl-beta-cyanoalanine	C05711	pos	244.0927	208316 ± 48705	131107 ± 19446	1.95	1.52	0.0418	down	0.875
Fluorouracil	C07649	neg	259.0284	5967 ± 1354	3989 ± 463	1.82	1.55	0.0484	down	0.9375
19-Hydroxytestosterone	C05294	pos	305.2102	16045 ± 3039	11206 ± 1164	1.53	1.60	0.0325	down	0.9375

m/z, mass-to-charge ratio; neg, negative ionization scanning mode; pos, positive ionization scanning mode; VIP, variable importance in projection; FC, fold change (mCtrl vs mVPA); up, the level of metabolite increased in mVPA group; down, the level of metabolite decreased in mVPA group; AUC, area under the curve (mCtrl vs mVPA).

Table 4. Relative abundance of 15 significant differential metabolites involved in KEGG pathway analysis between fCtrl and fVPA group (Mean ± SD).

Description	kegg_id	ESI mode	*m/z*	fCtrl	fVPA	VIP	FC	*p*-value	State	AUC
cis-Acetylacrylate	C07091	neg	227.0569	24604 ± 2401	14770 ± 4564	2.84	1.52	0.0194	down	0.9375
4-(Methylnitrosamino)-1-(3-pyridyl)-1-butanol	C19574	pos	419.2412	39016 ± 6026	22277 ± 2316	2.64	1.72	0.0022	down	1
Androstenedione	C00280	pos	287.2001	24223 ± 5563	13907 ± 2846	2.59	1.85	0.0218	down	0.9375
LysoPC(14:1(9Z))	C04230	neg	464.2762	32012 ± 5470	50873 ± 4095	2.46	0.63	0.0044	up	1
Brassicasterol	C08813	pos	421.3453	77492 ± 13803	124220 ± 11312	2.29	0.65	0.0044	up	1
Palmitoyl glucuronide	C03033	pos	441.2833	8607 ± 1274	13774 ± 3014	2.17	0.63	0.0288	up	0.875
D-1-Piperideine-2-carboxylic acid	C04092	neg	253.1191	4392 ± 1078	6522 ± 1038	2.16	0.57	0.0426	up	0.875
Allocholic acid	C00695	pos	431.2775	46091 ± 6581	30143 ± 5147	2.06	1.53	0.0144	down	0.9375
N-Acetyl-L-glutamate 5-semialdehyde	C01250	pos	174.0760	245595 ± 66216	350596 ± 13768	1.87	0.56	0.0494	up	1
Cyclohexylamine	C00571	pos	100.1124	11756 ± 2223	16922 ± 1034	1.82	0.56	0.0187	up	1
13S-hydroxyoctadecadienoic acid	C14762	pos	297.2418	853059 ± 168537	584732 ± 89237	1.77	1.67	0.0385	down	0.9375
N-Succinyl-2-amino-6-ketopimelate	C04462	neg	288.0728	71610 ± 11805	51309 ± 7824	1.72	1.55	0.0425	down	0.9375
Kynurenic acid	C01717	pos	190.0495	14068 ± 2717	19623 ± 1367	1.69	0.64	0.0219	up	1
3-Carbamoyl-2-phenylpropionaldehyde	C16587	neg	192.0658	25669 ± 4302	19095 ± 823	1.47	1.59	0.0222	down	1
Phytosphingosine	C12144	pos	318.2996	86653 ± 14864	113174 ± 6541	1.35	0.66	0.0360	up	0.9375

m/z, mass-to-charge ratio; neg, negative ionization scanning mode; pos, positive ionization scanning mode; VIP, variable importance in projection; FC, fold change (fCtrl vs fVPA); up, the level of metabolite increased in fVPA group; down, the level of metabolite decreased in fVPA group; AUC, area under the curve (fCtrl vs fVPA).

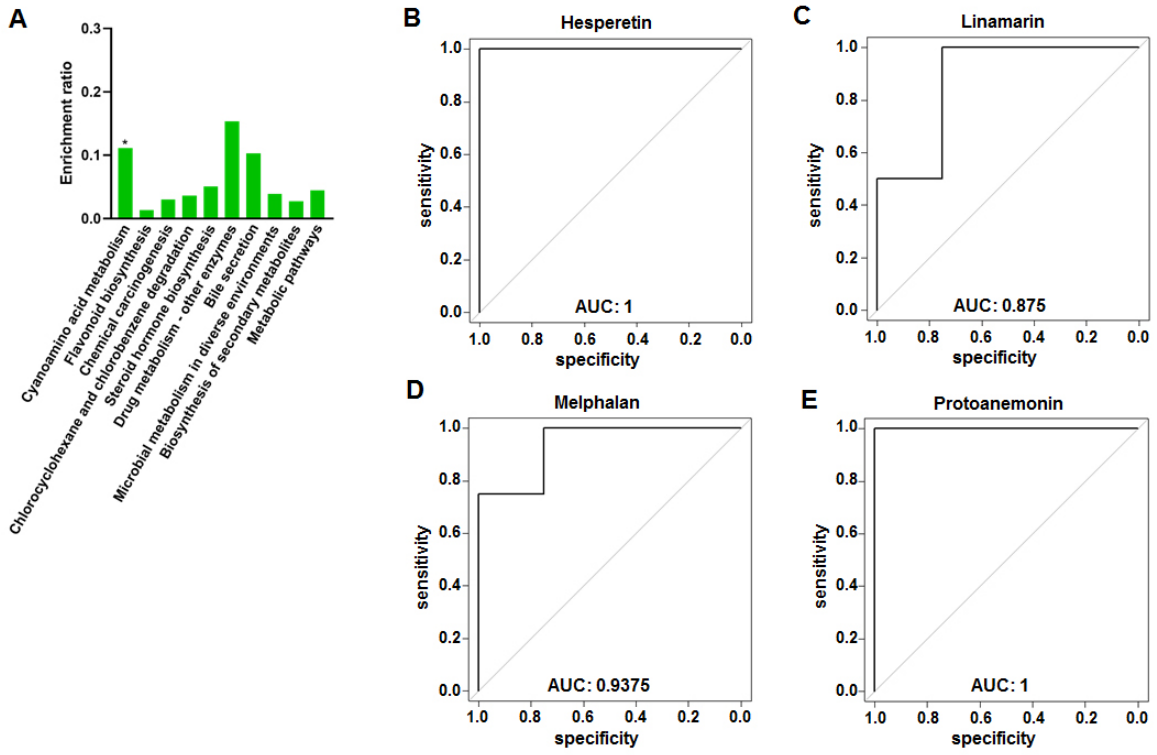

Fig. 3. KEGG analysis of fecal metabolites in male VPA rats. (A) KEGG pathway enrichment column chart in male VPA rats. The abscissa is the name of KEGG pathway. (B–E) Receiver operator characteristic curves of the four characteristic fecal metabolites. (B) Hesperetin. (C) Linamarin. (D) Melphalan. (E) Protoanemonin.

VPA rats. They found that the fecal samples of VPA rats showed reduced microbial richness as well as altered composition and metabolite potential of the microbial community. These features are similar to those in ASD individuals, suggesting that VPA rats might be suitable to detect the true variations in the GM and fecal metabolites of ASD. Based on these studies, we chose VPA rats as the animal model in the present study. We revealed the taxonomical characterization of the GM and the features of fecal metabolites in VPA rats and explored the underlying mechanism of ASD based on affected pathways in the KEGG database. Based on these data, we analyzed the correlation between characteristic GM and fecal metabolites in VPA rats. Sex-specific differences were also detected due to the substantial difference in morbidity between different sexes.

First, we analyzed the fecal samples by 16S rRNA gene sequencing. The richness and diversity of the GM showed no significant differences between VPA and Ctrl rats in either sex, which is different from a previous study [41]. PCoA showed that the overall composition of the GM was different between fVPA and fCtrl rats but not male rats. The results of characteristic genera and relative abundance showed noticeable sex-specific differences, suggesting that different probiotics might be used to treat male and female ASD patients. Interestingly the alteration of the F/B ratio was different between the different sexes, although the change was not statistically significant. Firmicutes and Bacteroidetes are the two most abundant bacterial phyla in the intestine. An altered F/B ratio is tightly related to ASD and obesity [24, 32, 46, 55–57], but the results in different studies are inconsistent. The incidence of obesity is significantly increased in ASD individuals [57–61], while the body weight of VPA rats is significantly lighter than that of Ctrl rats [49, 51]. Thus, it is difficult to speculate on the internal mechanism of the altered F/B ratio in the pathogenesis of ASD. Additional studies are needed in the future. In addition, correlation analysis showed a tight relationship between characteristic GM and characteristic fecal metabolites in both sexes of VPA rats, suggesting that the GM may influence the pathogenesis involving fecal metabolites.

In contrast to former studies, we used untargeted metabolomics to detect the differentially abundant fecal metabolites and analyzed them in the KEGG database. Between the mVPA and mCtrl groups, we detected 51 annotated differentially abundant fecal metabolites and identified 1 enriched KEGG pathway, namely, the pathway for cyanoamino acid metabolism. Seven characteristic fecal metabolites were determined to distinguish male VPA rats. Between the fVPA and fCtrl groups, 124 annotated differentially abundant fecal metabolites were detected with no enriched KEGG pathways being identified. Fifteen characteristic fecal metabolites to distinguish female VPA rats were determined. The enriched KEGG pathways and the characteristic fecal metabolites showed obvious sex-specific dif-

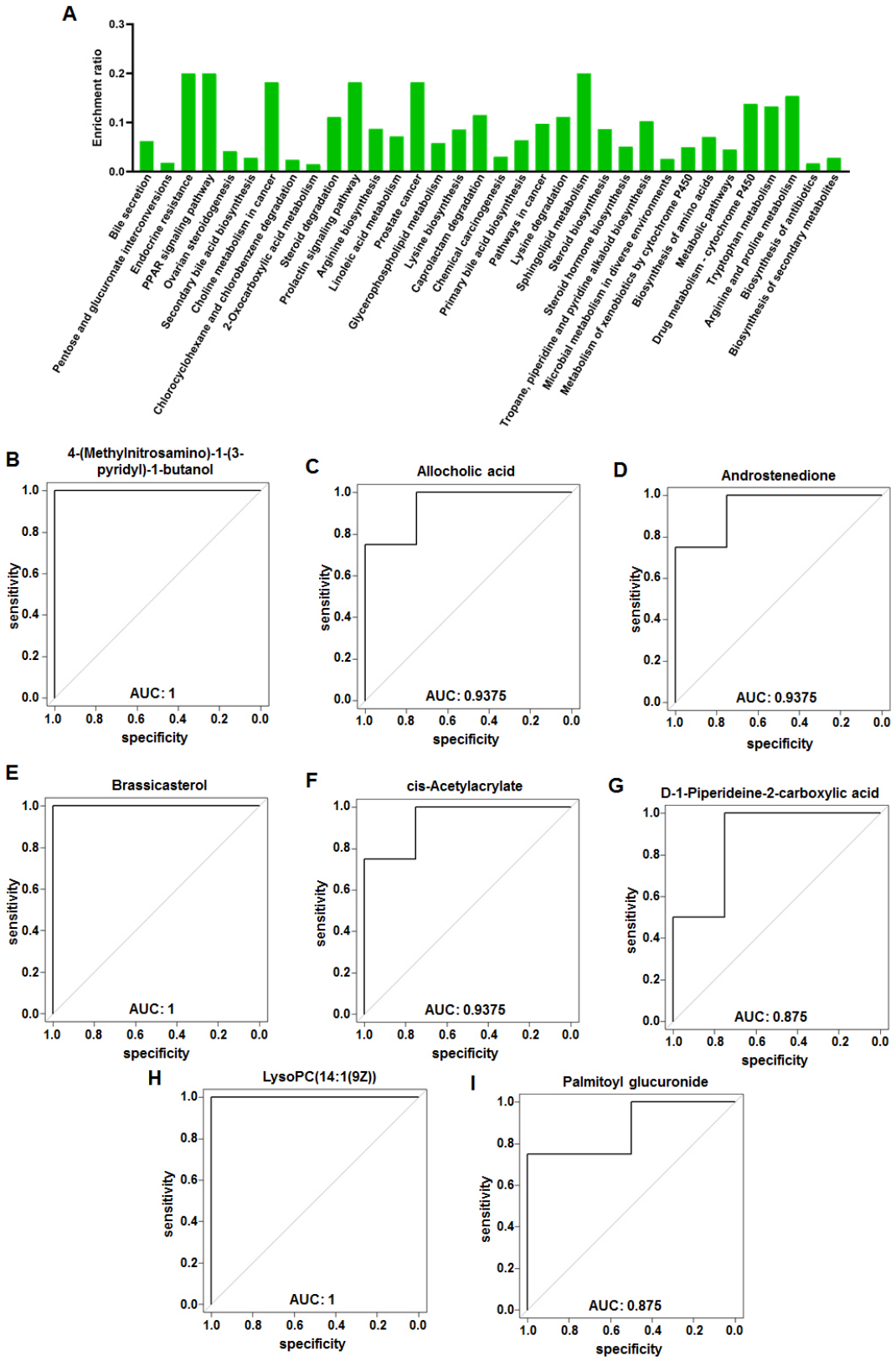

Fig. 4. KEGG analysis of fecal metabolites in female VPA rats. (A) KEGG pathway enrichment column chart in female VPA rats. The abscissa is the name of KEGG pathway. (B–I) Receiver operator characteristic curves of the eight characteristic fecal metabolites. (B) 4-(Methylnitrosamino)-1-(3-pyridyl)-1-butanol. (C) Allocholic acid. (D) Androstenedione. (E) Brassicasterol. (F) cis-Acetylacrylate. (G) D-1-Piperideine-2-carboxylic acid. (H) LysoPC(14:1(9Z)). (I) Palmitoyl glucuronide.

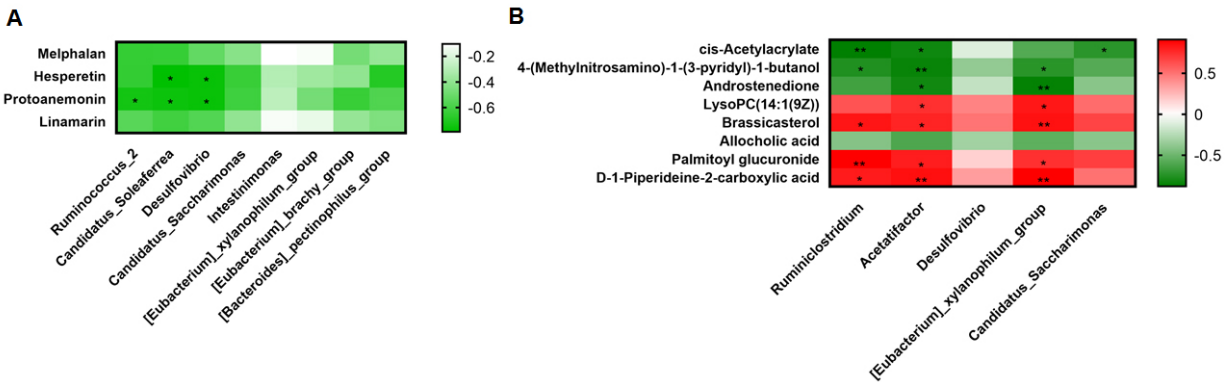

Fig. 5. Correlation analysis of gut microbiota and fecal metabolites in male and female VPA rats. (A) Correlation heatmap between sixteen characteristic fecal metabolites and eight characteristic genera in abundance in male VPA rats. (B) Correlation heatmap between sixteen characteristic fecal metabolites and eight characteristic genera in abundance in female VPA rats. The legend on the right is the color range of different R values. The abscissa represents characteristic genera, and the ordinate represents characteristic fecal metabolites. * $p < 0.05$, ** $p < 0.01$, *** $p < 0.001$.

ferences. Some results had been reported previously. For example, hesperetin was shown to ameliorate social behavior deficits and oxido-inflammatory stress in a rat autism model [62]. Alteration of bile acid metabolism has been shown to be associated with gastrointestinal dysfunction in BTBR mice, a mouse model of autism [63]. Correlation analysis showed a tight relationship between characteristic GM and characteristic fecal metabolites in both sexes of VPA rats, suggesting that the GM may influence the pathogenesis involving fecal metabolites. The abundance of *Candidatus_Soleaferrea* and *Desulfovibrio* negatively correlated with that of hesperetin, suggesting that these 2 genera might exacerbate autism-like behavior. Tomova *et al.* and Zurita *et al.* [21, 25] reported that the abundance of *Desulfovibrio* is significantly elevated in the fecal samples of children with ASD, which is consistent with our results. However, in most studies, only male animals were involved. These results might not hold true in female ASD animal models or female ASD patients. In the future, the above enriched KEGG pathways and characteristic metabolites might be research directions for exploring ASD therapy. Both male and female patients or animal models should be involved and analyzed separately.

This study has some limitations. First, the number of animals included in our study was slightly small (n = 4). Second, in this study, we analyzed sex-specific differences, not sex-related differences, in the GM and fecal metabolites of VPA rats. That is, we did not analyze the differences between sexes. On the basis of our knowledge, it is suggested that differential metabolites should be screened between two groups. Sex-related alterations of the GM and fecal metabolites in patients with ASD or animal models of ASD might be analyzed in the future when differential metabolites could be screened among 3 or more groups. Finally, the omics results need to be verified by further research, such as molecular biology studies.

6. Conclusions

In general, we used 16S rRNA gene sequencing and untargeted metabolomics to explore the characteristics of fecal metabolites and the GM in male and female VPA rats. Dysbacteriosis existed in the fecal samples of both male and female VPA rats, with sex-specific differences. The specific alteration of the GM and fecal metabolites may play a crucial role in the pathogenesis of ASD. This is the first study focusing on sex-specific differences in fecal metabolites and KEGG pathways in VPA-induced rat autism model. According to our results, the mechanism of ASD might be very different between male and female patients, suggesting that in future ASD studies, both male and female patients or animal models should be involved and analyzed separately. ASD therapy might be different between sexes in the future.

7. Author contributions

YYG, YH and JQ designed the study; YNC, JJL and SBZ performed 16S rRNA gene sequencing and untargeted metabolomics; BZ and YZ analyzed the experiments data and graphed. YH and JQ approved the manuscript; YYG finalized the manuscript.

8. Ethics approval and consent to participate

The animal experimental procedures were approved by Animal Care and Use Committee of Peking University People's Hospital (2019PHE007).

9. Acknowledgment

We express our appreciation to all members of Laboratory Animal Center of Peking University People's Hospital for their assistance with maintenance of rats.

10. Funding

This work was supported by Natural Science Foundation of Beijing (S170003) and Beijing Municipal Key Clinical Specialty Program (2018).

11. Conflict of interest

The authors declare no conflict of interest.

12. References

[1] Kim JY, Son MJ, Son CY, Radua J, Eisenhut M, Gressier F, *et al*. Environmental risk factors and biomarkers for autism spectrum disorder: an umbrella review of the evidence. The Lancet Psychiatry. 2019; 6: 590–600.

[2] Rogozin IB, Gertz EM, Baranov PV, Poliakov E, Schaffer AA. Genome-Wide Changes in Protein Translation Efficiency are Associated with Autism. Genome Biology and Evolution. 2018; 10: 1902–1919.

[3] Hallmayer J. Genetic Heritability and Shared Environmental Factors among Twin Pairs with Autism. Archives of General Psychiatry. 2011; 68: 1095.

[4] Bhat S, Acharya UR, Adeli H, Bairy GM, Adeli A. Autism: cause factors, early diagnosis and therapies. Reviews in the Neurosciences. 2015; 25: 841–850.

[5] Dietert RR, Dietert JM, Dewitt JC. Environmental risk factors for autism. Emerging Health Threats Journal. 2011; 4: 7111.

[6] Varghese M, Keshav N, Jacot-Descombes S, Warda T, Wicinski B, Dickstein DL, *et al*. Autism spectrum disorder: neuropathology and animal models. Acta Neuropathologica. 2018; 134: 537–566.

[7] Christensen DL, Baio J, Van Naarden Braun K, Bilder D, Charles J, Constantino JN, *et al*. Prevalence and Characteristics of Autism Spectrum Disorder among Children Aged 8 Years–Autism and Developmental Disabilities Monitoring Network, 11 Sites, United States, 2012. Morbidity and Mortality Weekly Report. Surveillance Summaries. 2016; 65: 1–23.

[8] Werling DM, Geschwind DH. Sex differences in autism spectrum disorders. Current Opinion in Neurology. 2013; 26: 146–153.

[9] Quigley EMM. Microbiota-Brain-Gut Axis and Neurodegenerative Diseases. Current Neurology and Neuroscience Reports. 2018; 17: 94.

[10] Cryan JF, Dinan TG. Mind-altering microorganisms: the impact of the gut microbiota on brain and behavior. Nature Reviews Neuroscience. 2012; 13: 701–712.

[11] Zierer J, Jackson MA, Kastenmüller G, Mangino M, Long T, Telenti A, *et al*. The fecal metabolome as a functional readout of the gut microbiome. Nature Genetics. 2018; 50: 790–795.

[12] El Aidy S, Stilling R, Dinan TG, Cryan JF. Microbiome to Brain: Unravelling the Multidirectional Axes of Communication. Microbial Endocrinology: Interkingdom Signaling in Infectious Disease and Health. 2016; 21: 301–336.

[13] Diaz Heijtz R, Wang S, Anuar F, Qian Y, Björkholm B, Samuelsson A, *et al*. Normal gut microbiota modulates brain development and behavior. Proceedings of the National Academy of Sciences of the United States of America. 2011; 108: 3047–3052.

[14] Fiorentino M, Sapone A, Senger S, Camhi SS, Kadzielski SM, Buie TM, *et al*. Blood-brain barrier and intestinal epithelial barrier alterations in autism spectrum disorders. Molecular Autism. 2017; 7: 49.

[15] Dalton N, Chandler S, Turner C, Charman T, Pickles A, Loucas T, *et al*. Gut permeability in autism spectrum disorders. Autism Research. 2015; 7: 305–313.

[16] Chaidez V, Hansen RL, Hertz-Picciotto I. Gastrointestinal problems in children with autism, developmental delays or typical development. Journal of Autism and Developmental Disorders. 2014; 44: 1117–1127.

[17] Adams JB, Johansen LJ, Powell LD, Quig D, Rubin RA. Gastrointestinal flora and gastrointestinal status in children with autism–comparisons to typical children and correlation with autism severity. BMC Gastroenterology. 2011; 11: 22.

[18] de Magistris L, Familiari V, Pascotto A, Sapone A, Frolli A, Iardino P, *et al*. Alterations of the intestinal barrier in patients with autism spectrum disorders and in their first-degree relatives. Journal of Pediatric Gastroenterology and Nutrition. 2011; 51: 418–424.

[19] Buie T, Campbell DB, Fuchs GJ, Furuta GT, Levy J, Vandewater J, *et al*. Evaluation, diagnosis, and treatment of gastrointestinal disorders in individuals with ASDs: a consensus report. Pediatrics. 2010; 125: S1–S18.

[20] Campbell DB, Buie TM, Winter H, Bauman M, Sutcliffe JS, Perrin JM, *et al*. Distinct genetic risk based on association of MET in families with co-occurring autism and gastrointestinal conditions. Pediatrics. 2009; 123: 1018–1024.

[21] Tomova A, Soltys K, Repiska G, Palkova L, Filcikova D, Minarik G, *et al*. Specificity of gut microbiota in children with autism spectrum disorder in Slovakia and its correlation with astrocytes activity marker and specific behavioral patterns. Physiology & Behavior. 2020; 214: 112745.

[22] Ho LKH, Tong VJW, Syn N, Nagarajan N, Tham EH, Tay SK, *et al*. Gut microbiota changes in children with autism spectrum disorder: a systematic review. Gut Pathogens. 2020; 12: 6.

[23] Bezawada N, Phang T, Hold G, Hansen R. Autism Spectrum Disorder and the Gut Microbiota in Children: a Systematic Review. Annals of Nutrition and Metabolism. 2020; 76: 16–29.

[24] Ahmed SA, Elhefnawy AM, Azouz HG, Roshdy YS, Ashry MH, Ibrahim AE, *et al*. Study of the gut Microbiome Profile in Children with Autism Spectrum Disorder: A Single Tertiary Hospital Experience. Journal of Molecular Neuroscience. 2020; 70: 887–896.

[25] Zurita MF, Cárdenas PA, Sandoval ME, Peña MC, Fornasini M, Flores N, *et al*. Analysis of gut microbiome, nutrition and immune status in autism spectrum disorder: a case-control study in Ecuador. Gut Microbes. 2020; 11: 453–464.

[26] Wang M, Wan J, Rong H, He F, Wang H, Zhou J, *et al*. Alterations in Gut Glutamate Metabolism Associated with Changes in Gut Microbiota Composition in Children with Autism Spectrum Disorder. MSystems. 2019, 4: e00321–18.

[27] Sun H, You Z, Jia L, Wang F. Autism spectrum disorder is associated with gut microbiota disorder in children. BMC Pediatrics. 2019; 19: 516.

[28] Ristori MV, Quagliariello A, Reddel S, Ianiro G, Vicari S, Gasbarrini A, *et al*. Autism, Gastrointestinal Symptoms and Modulation of Gut Microbiota by Nutritional Interventions. Nutrients. 2019; 11: 2812.

[29] Ma B, Liang J, Dai M, Wang J, Luo J, Zhang Z, *et al*. Altered Gut Microbiota in Chinese Children With Autism Spectrum Disorders. Frontiers in Cellular and Infection Microbiology. 2019; 9: 40.

[30] Liu S, Li E, Sun Z, Fu D, Duan G, Jiang M, *et al*. Altered gut microbiota and short chain fatty acids in Chinese children with autism spectrum disorder. Scientific Reports. 2019; 9: 287.

[31] Liu F, Li J, Wu F, Zheng H, Peng Q, Zhou H. Altered composition and function of intestinal microbiota in autism spectrum disorders: a systematic review. Translational Psychiatry. 2019; 9: 43.
[32] Coretti L, Paparo L, Riccio MP, Amato F, Cuomo M, Natale A, *et al*. Gut Microbiota Features in Young Children With Autism Spectrum Disorders. Frontiers in Microbiology. 2018; 9: 3146.
[33] Coretti L, Cristiano C, Florio E, Scala G, Lama A, Keller S, *et al*. Sex-related alterations of gut microbiota composition in the BTBR mouse model of autism spectrum disorder. Scientific Reports. 2018; 7: 45356.
[34] de Theije CGM, Wopereis H, Ramadan M, van Eijndthoven T, Lambert J, Knol J, *et al*. Altered gut microbiota and activity in a murine model of autism spectrum disorders. Brain, Behavior, and Immunity. 2014; 37: 197–206.
[35] Sharon G, Cruz NJ, Kang D, Gandal MJ, Wang B, Kim Y, *et al*. Human Gut Microbiota from Autism Spectrum Disorder Promote Behavioral Symptoms in Mice. Cell. 2019; 177: 1600–1618.e17.
[36] De Angelis M, Piccolo M, Vannini L, Siragusa S, De Giacomo A, Serrazzanetti DI, *et al*. Fecal microbiota and metabolome of children with autism and pervasive developmental disorder not otherwise specified. PLoS ONE. 2014; 8: e76993.
[37] Wang L, Christophersen CT, Sorich MJ, Gerber JP, Angley MT, Conlon MA. Elevated fecal short chain fatty acid and ammonia concentrations in children with autism spectrum disorder. Digestive Diseases and Sciences. 2012; 57: 2096–2102.
[38] Israelyan N, Margolis KG. Reprint of: Serotonin as a link between the gut-brain-microbiome axis in autism spectrum disorders. Pharmacological Research. 2019; 140: 115–120.
[39] Yano JM, Yu K, Donaldson GP, Shastri GG, Ann P, Ma L, *et al*. Indigenous bacteria from the gut microbiota regulate host serotonin biosynthesis. Cell. 2015; 161: 264–276.
[40] Yu M, Jia H, Zhou C, Yang Y, Zhao Y, Yang M, *et al*. Variations in gut microbiota and fecal metabolic phenotype associated with depression by 16S rRNA gene sequencing and LC/MS-based metabolomics. Journal of Pharmaceutical and Biomedical Analysis. 2017; 138: 231–239.
[41] Barrett CE, Hennessey TM, Gordon KM, Ryan SJ, McNair ML, Ressler KJ, *et al*. Developmental disruption of amygdala transcriptome and socioemotional behavior in rats exposed to valproic acid prenatally. Molecular Autism. 2018; 8: 42.
[42] Wang C, Lin H, Chan Y, Gean P, Yang YK, Chen PS. 5-HT1a-receptor agonist modified amygdala activity and amygdala-associated social behavior in a valproate-induced rat autism model. The International Journal of Neuropsychopharmacology. 2014; 16: 2027–2039.
[43] Liu F, Horton-Sparks K, Hull V, Li RW, Martínez-Cerdeño V. The valproic acid rat model of autism presents with gut bacterial dysbiosis similar to that in human autism. Molecular Autism. 2018; 9: 61.
[44] Dai Y, Zhang H, Schön M, Böckers TM, Han S, Han J, *et al*. Neonatal Oxytocin Treatment Ameliorates Autistic-Like Behaviors and Oxytocin Deficiency in Valproic Acid-Induced Rat Model of Autism. Frontiers in Cellular Neuroscience. 2019; 12: 355.
[45] Schneider T, Przewłocki R. Behavioral alterations in rats prenatally exposed to valproic acid: animal model of autism. Neuropsychopharmacology. 2005; 30: 80–89.
[46] Niu M, Li Q, Zhang J, Wen F, Dang W, Duan G, *et al*. Characterization of Intestinal Microbiota and Probiotics Treatment in Children with Autism Spectrum Disorders in China. Frontiers in Neurology. 2019; 10: 1084.
[47] Zhou L, Ni Z, Yu J, Cheng W, Cai Z, Yu C. Correlation Between Fecal Metabolomics and Gut Microbiota in Obesity and Polycystic Ovary Syndrome. Frontiers in Endocrinology. 2020; 11: 628.
[48] Ni Z, Sun S, Bi Y, Ding J, Cheng W, Yu J, *et al*. Correlation of fecal metabolomics and gut microbiota in mice with endometriosis. American Journal of Reproductive Immunology. 2020; 84: e13307.
[49] Kanehisa M, Furumichi M, Tanabe M, Sato Y, Morishima K. KEGG: new perspectives on genomes, pathways, diseases and drugs. Nucleic Acids Research. 2017; 45: D353–D361.
[50] Foley KA, MacFabe DF, Vaz A, Ossenkopp K, Kavaliers M. Sexually dimorphic effects of prenatal exposure to propionic acid and lipopolysaccharide on social behavior in neonatal, adolescent, and adult rats: implications for autism spectrum disorders. International Journal of Developmental Neuroscience. 2015; 39: 68–78.
[51] Chaliha D, Albrecht M, Vaccarezza M, Takechi R, Lam V, Al-Salami H, *et al*. A Systematic Review of the Valproic-Acid-Induced Rodent Model of Autism. Developmental Neuroscience. 2020; 42: 12–48.
[52] Nicolini C, Fahnestock M. The valproic acid-induced rodent model of autism. Experimental Neurology. 2017; 299: 217–227.
[53] Roullet FI, Lai JKY, Foster JA. In utero exposure to valproic acid and autism–a current review of clinical and animal studies. Neurotoxicology and Teratology. 2013; 36: 47–56.
[54] Sacco R, Curatolo P, Manzi B, Militerni R, Bravaccio C, Frolli A, *et al*. Principal pathogenetic components and biological endophenotypes in autism spectrum disorders. Autism Research. 2011; 3: 237–252.
[55] Zhang M, Ma W, Zhang J, He Y, Wang J. Analysis of gut microbiota profiles and microbe-disease associations in children with autism spectrum disorders in China. Scientific Reports. 2019; 8: 13981.
[56] Strati F, Cavalieri D, Albanese D, De Felice C, Donati C, Hayek J, *et al*. New evidence on the altered gut microbiota in autism spectrum disorders. Microbiome. 2017; 5: 1–14.
[57] John GK, Mullin GE. The Gut Microbiome and Obesity. Current Oncology Reports. 2017; 18: 45.
[58] Pham D, Silver S, Haq S, Hashmi SS, Eissa M. Obesity and Severe Obesity in Children with Autism Spectrum Disorder: Prevalence and Risk Factors. Southern Medical Journal. 2020; 113: 168–175.
[59] McCoy SM, Morgan K. Obesity, physical activity, and sedentary behaviors in adolescents with autism spectrum disorder compared with typically developing peers. Autism. 2020; 24: 387–399.
[60] Li Y, Xie X, Lei X, Li Y, Lei X. Global prevalence of obesity, overweight and underweight in children, adolescents and adults with autism spectrum disorder, attention-deficit hyperactivity disorder: a systematic review and meta-analysis. Obesity Reviews. 2020; 21: e13123.
[61] Healy S, Aigner CJ, Haegele JA. Prevalence of overweight and obesity among us youth with autism spectrum disorder. Autism. 2019; 23: 1046–1050.
[62] Khalaj R, Hajizadeh Moghaddam A, Zare M. Hesperetin and it nanocrystals ameliorate social behavior deficits and oxido-inflammatory stress in rat model of autism. International Journal of Developmental Neuroscience. 2018; 69: 80–87.
[63] Golubeva AV, Joyce SA, Moloney G, Burokas A, Sherwin E, Arboleya S, *et al*. Microbiota-related Changes in Bile Acid & Tryptophan Metabolism are Associated with Gastrointestinal Dysfunction in a Mouse Model of Autism. EBioMedicine. 2017; 24: 166–178.

Supplementary material: Supplementary material associated with this article can be found, in the online version, at https://www.imrpress.com/journal/FBL/26/12/10.52586/5051.

Abbreviations: 5-HT, 5-hydroxytryptamine; ASD, autism spectrum disorder; AUC, area under the curve; CNS, center nervous system; Ctrl, control; DNA, deoxyribonucleic acid; F/B, Firmicutes/Bacteroides; FC, fold change;

FDR, false discovery rate; GI, gastrointestinal; GM, gut microbiota; KEGG, Kyoto Encyclopedia of Genes and Genomes; UHPLC-MS, ultra-high-performance liquid chromatography-mass spectrometry; LEfSe, linear discriminant analysis effect size; NS, normal saline; OPLS-DA, orthogonal partial least squares discrimination analysis; OTU, operational taxonomic unit; PCA, principal component analysis; PCoA, principal coordinate analysis; PCR, polymerase chain reaction; PND, postnatal day; QC, quality control; ROC, receiver operator characteristic; rRNA, ribosomal ribonucleic acid; VIP, variable important in projection; VPA, valproic acid.

Keywords: Autism spectrum disorder; Valproic acid; Gut microbiota; Fecal metabolomics; Sex-specific differences

Send correspondence to:

Ying Han, Department of Pediatrics, Peking University First Hospital, 100034 Beijing, China, E-mail: hanying1568@bjmu.edu.cn

Jiong Qin, Department of Pediatrics, Peking University People's Hospital, 100044 Beijing, China, E-mail: qinjiong@pkuph.edu.cn